sciendo
ISSN 1335-8871
MEASUREMENT SCIENCE REVIEW
Journal homepage: https://content.sciendo.com

Review of Measurement Techniques of Hydrocarbon Flame Equivalence Ratio and Applications of Machine Learning

Hao Yang[1], Yuwen Fu[2], Jiansheng Yang[1]

[1] *The Electrical Engineering College, Guizhou University, Guiyang 550025, China, jsyang3@gzu.edu.cn*
[2] *Guizhou Communication Polytechnic, Guiyang 550025, China*

Flame combustion diagnostics is a technique that uses different methods to diagnose the flame combustion process and study its physical and chemical basis. As one of the most important parameters of the combustion process, the flame equivalence ratio has a significant influence on the entire flame combustion, especially on the combustion efficiency and the emission of pollutants. Therefore, the measurement of the flame equivalence ratio has a huge impact on efficient combustion and environment protection. In view of this, several effective measuring methods were proposed, which were based on the different characteristics of flames radicals such as spectral properties. With the rapid growth of machine learning, more and more scholars applied it in the combustion diagnostics due to the excellent ability to fit parameters. This paper presents a review of various measuring techniques of hydrocarbon flame equivalent ratio and the applications of machine learning in combustion diagnostics, finally making a brief comparison between different measuring methods.

Keywords: Combustion diagnostics; measuring techniques; equivalence ratio; multispectral imaging; machine learning.

1. INTRODUCTION

Combustion diagnostics is one of the main challenges the combustion industry faces, and thus the improvement of combustion diagnostics technology has a huge impact on the detection of combustion rates, stability, and the emission of the pollutants. The combustion rate, stability depends to a large extent on the setting of the combustion conditions. Flame equivalence ratio [1] is a parameter which measures the degree of mixture of fuel and oxidizer, and the equivalence ratio of hydrocarbon flame is defined as (1).

$$\Phi = \frac{(Air/Fuel)_{stio}}{(Air/Fuel)_{real}} \quad (1)$$

as shown in (1), $(Air/Fuel)_{stio}$ represents the stoichiometric ratio of air to fuel. When Φ is 1, it is complete combustion. When $\Phi > 1$, it is rich combustion state. When $\Phi < 1$, it is lean combustion state. The equivalence ratio is one of the most important factors which affect the combustion state and the generation of pollutants, among the variables that can be monitored throughout the combustion process. The relationship between combustion efficiency and flame equivalence ratio is inextricably linked. Therefore, the study of equivalence ratio helps in enhancing the understanding of fuel properties and optimizing burner construction for energy saving and pollutant emission reduction, which is meaningful and necessary for combustion diagnostics.

This paper focuses on the measurement of flame equivalence ratio from passive and active measuring methods, as shown in Fig.1. Flame combustion is a self-luminous process. The equivalence ratio is generally measured by detecting the concentration or chemiluminescence intensities of the radicals, such as OH^*, CH^*, and C_2^*. As in [2], [3], the flames have the OH* chemiluminescence peak near 310 nm, and the peak intensity increases with the increasing of the equivalence ratio. Thus OH^* chemiluminescence intensity can be applied to indicate the global equivalence ratio. It was found that the chemiluminescence intensity of CH^* and C_2^* depended on the equivalence ratio non-monotonically in [4]. Clark [5] demonstrated that the chemiluminescence intensity of flame radicals CH^* and C_2^* can be applied to indicate the equivalence ratio of the flame. Haber [6] also confirmed that the CH^*/C_2^* chemiluminescence ratio can be used to approximate the equivalence ratio. The passive measuring method is the use of different methods to detect the chemiluminescence intensity of radicals in the combustion process, and the equivalence ratio can be indicated according to the radical chemiluminescence intensities. The active measuring method applies an external excitation, such as laser, etc. to excite the atom or molecule in the flame to transition to a higher energy level, and the atom or molecule releases a corresponding spectral signal when it returns to a lower energy level. In that case, the original measurement of flame radical spectral intensity is then transformed into a

DOI: 10.2478/msr-2022-0016

measurement of the spectral signal concentration emitted by the particles after excitation. The rapid development of machine learning has provided a new technical route for combustion diagnostics. Compared with the traditional manual construction of models for different flames based on a single feature, machine learning has shown the excellent classification performance and the generalization ability under the condition of high-dimensional features. At this stage, machine learning has been widely used in fuel identification, combustion efficiency prediction, combustion exergy prediction and pollutant emission prediction in combustion diagnostics field. This paper presents the applications of machine learning in combustion diagnostics.

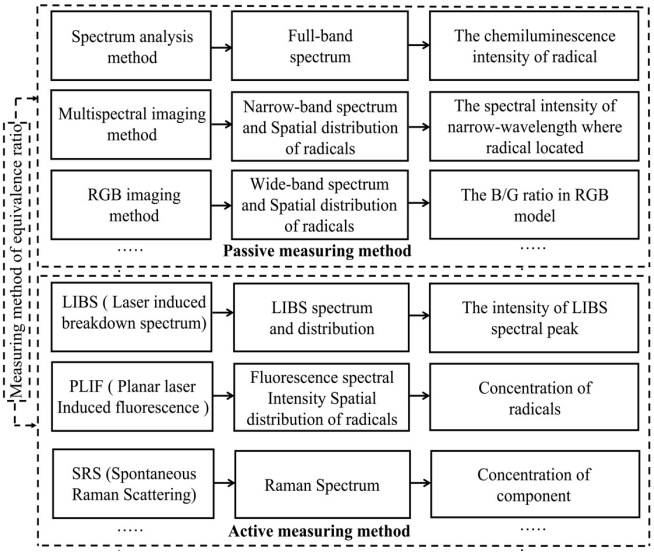

Fig.1. Methods of measuring the equivalence ratio.

In recent decades, scholars have studied the radicals in flame combustion from several perspectives and proposed many methods of flame equivalence ratio measurement. This paper will introduce the different measuring methods of flame equivalence ratio and the applications of machine learning in combustion diagnostics field, finally providing an outlook on the future development.

2. PASSIVE MEASURING METHODS

The passive measuring methods mainly include the spectral analysis method, the multispectral imaging method, and the RGB imaging method. Spectral analysis method applies a spectrometer to obtain the radical spectral intensity precisely. The spectrometer method can obtain the complete spectral information of the radicals, but it lacks the spatial information of the radicals, in which case the spatial distribution of radicals cannot be analyzed. In addition, the spectrum analysis method relies on the flames that are free of broadband soot luminescence.

To obtain the spatial information of the flame, some scholars apply the multispectral imaging method to detect the flame radicals. Several methods were applied to record the image in multispectral imaging: (1) Separation method: According to the different refractive indices of light in different wavelengths, mapping different parts of the spectrum to the top parts of the CCD chip [7]. Mapping different parts of spectrum onto CCD chips is one of the more accurate among multispectral imaging methods, but again the cost is the highest. Also using the principle of refraction of light so that different bands of light can be mapped at different locations in the same plane, a high precision optical lens can be taken into consideration to refract the flame to a plane. But the disadvantage of the optical lens is that a lot of calibration work needs to be done before imaging the flame, and the optical path is difficult to determine. (2) Several cameras method: Adding the filters of each part of the spectrum to different cameras. The method is most used in the multispectral imaging method, in which the advantages are that radical images in multiple wavelengths can be processed simultaneously to obtain the spatial and spectral information of flame radicals at the same moment. However, because it involves simultaneous shooting by different cameras, it is necessary to ensure that the error in shooting time is small, as well as the need for precise matching of images of different bands of the same flame at a later stage. (3) Consecutive method: Adding the filters of each part of the spectrum to a camera and imaging one after one [8]. Compared with (1) and (2), the method is the simplest, but the error is rather big due to the assumption that the flame remains steady. Multispectral imaging method obtains both the luminous intensity and two-dimensional spatial distribution of radicals, and thus the local equivalence ratio can be measured. But the use of narrow-band filters leads to some deficiencies in spectral accuracy compared to the spectrometer method. For example, if a 430 nm (± 10 nm) filter is used, the radical spectral information obtained is the integral of the spectral intensity in the band of 420-440. Based on this basis, there is a common compromise in which a spectrometer is combined with a camera. The spatial dimension is resolved by camera, and the other dimension of spectrometer resolves the spectrum [9]. The compromise method works well if the visualization is limited to a specific line, or if the geometry of the flame is essentially 1D.

RGB imaging method was developed by Huang et al. [10], who found that the chemiluminescence intensity of CH* and C2* in the methane flame was well matched with the median intensity of the B and G channels, and thus the ratio of the intensity of the B and G channels could be used to approximate the equivalence ratio. Yang et al. [11] improved the color-modelled CH* and C2* measurement using a digital color camera, in which case the mathematical model for detecting the flame equivalence ratio was optimized by calibrating the spectral corresponding function of the camera. The RGB imaging method is the simplest among the passive measuring methods, but it loses a lot of sensitivity to the variation of radical chemiluminescence peak. To be precise, each pixel in color image is equipped either with a R, G or B filter and the color image is interpolated from this information, which contains a lot of redundant information. Thus, the RGB imaging method is not sensitive to the variation of radical chemiluminescence peak. An additional drawback is that the OH* chemiluminescence intensity cannot be detected by the RGB imaging method, because the RGB wavelength does not cover the wavelength where the OH* is located.

A. Spectral analysis method

Flames are the product of a violent oxidation reaction between a fuel and an oxidant, which can be divided into premixed and diffusion flames, depending on whether the fuel and oxidant are premixed or not. During the combustion of a flame, the light wave signal is continuously radiated from it, covering the ultraviolet wavelength and infrared wavelength [12]. The spectral signal can be detected by a spectrometer which can analyze the whole spectral information of the flame detected as shown in Fig.2. The setup of the spectrum method for equivalence ratio measurement consists of a spectrometer and optical fibers, where the optical fibers are used to transmit the spectral information of the flame in the burner to the spectrograph. For the spectral analysis method, the accuracy depends mainly on the range and resolution of the spectrograph.

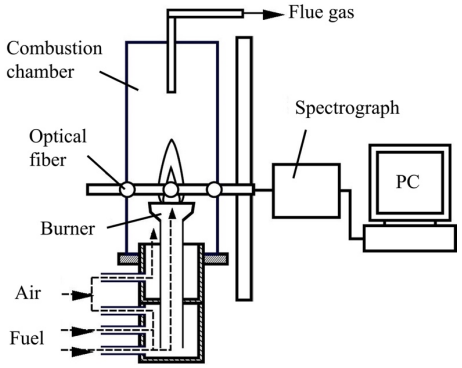

Fig.2. The setup of spectrum analysis method for equivalence ratio measurement. [9]

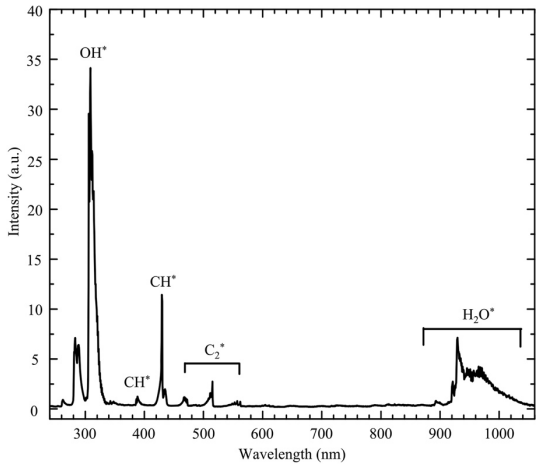

Fig.3. Radiation spectrum of a CH_4/O_2 flame with 30 % H_2 addition. [13].

The main process of measuring the flame equivalence ratio by the spectral analysis method consists of two parts. Firstly, the optical fibers are put on the flame area where the equivalence ratio needs to be measured. Then, the spectral signal transmitted from optical fibers can be analyzed by a spectrometer, in which case the entire spectral information of the area detected can be obtained. And spectral intensities of the different radicals, which can approximate the equivalence ratio, can be obtained. According to the reference [5], the equivalence ratio of the flame area detected can be indicated with the spectral intensities of the specific flame radicals, such as OH^*, CH^*, and C_2^*. The radiation spectrum of a CH_4/O_2 flame with 30 % H_2 addition is shown as Fig.3. It makes clear that the detailed spectral intensity of the specific radicals can be obtained. For hydrocarbon fuels, the main radicals for their chemiluminescence are OH^*, CH^*, and C_2^*. The spectral distribution can be derived clearly from the radiation spectrum of the flame. The OH^*, CH^* and C_2^* chemiluminescence are emitted at 310 nm, 430 nm, and 516.5 nm (dominative emissive band peak in the C_2^* Swan system), respectively, and OH^* intensity has a stronger chemiluminescence intensity compared with CH^* and $C2^*$. In general terms, the radicals OH^*, CH^* and $C2^*$ are commonly applied to equivalence ratio due to the stronger signal intensity compared with others.

The correlations between the chemiluminescence intensity ratios and equivalence ratio in CH_4-Air premixed flames are shown in Fig.4. Seen in Fig.4., the C_2^*/OH^* ratio increases more sensitively with the increase of the equivalence ratio, but it goes down towards the condition (Φ =1.35 - 1.5). Compared with C_2^*/OH^* ratio, OH^*/CH^* ratio lacks some sensitivity, but it goes down linearly to the increase of the equivalence ratio. The comparison demonstrated that different radical chemiluminescence ratios can be employed, according to different requirements. Manuel et al. [14] proposed an equivalence ratio measurement technique based on the spectrum analysis method for the fluctuations in a lean premixed kerosene combustor. To investigate the correlation between radical chemiluminescence intensity and equivalence ratio, the spectrometer was employed to detect the radical chemiluminescence intensity. It was found that $CH^*/C2^*$ ratio varied with equivalence ratio variation, which illustrated that $CH^*/C2^*$ ratio can be applied to indicate the equivalence ratio of fluctuations in a lean premixed kerosene combustor.

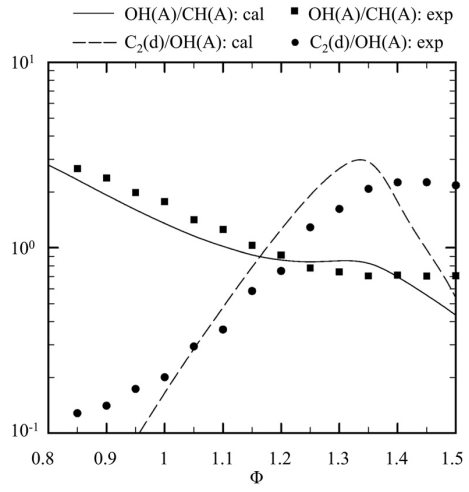

Fig.4. The correlations between the chemiluminescence intensity ratio and equivalence ratio in CH_4-Air premixed flames. [4]

The spectrum method is also employed in other areas of combustion diagnostics. Bedard et al. [15] extracted the temporal evolution of chemiluminescent species by analyzing the flame emission spectrum with a fiber optic probe, which

investigated the relationship between chemiluminescence species and heat release rate of the flame, enabling chemiluminescence to be a diagnostic parameter in combustion instability prediction.

Spectral analysis method provides precise radical chemiluminescence intensity and performs sensitively to the radical chemiluminescence variation. A drawback is that spatial information of flames is unavailable to the spectral analysis method, and thus the flame spatial structure cannot be analyzed. Therefore, some scholars proposed the multispectral imaging method to obtain the spatial information of flame radicals to further study the flame structure.

B. Multispectral imaging method

The flame radical chemiluminescence is the spontaneous spectral radiation over a specific wavelength, and the radicals applied commonly to equivalence ratio measurement are OH^*, CH^*, and $C2^*$. The spectrum peaks of OH^*, CH^* and $C2^*$ in hydrocarbon flames are nearly at 310 nm, 430 nm, 516 nm. Thus, serval multispectral imaging methods can be applied to record the radicals at different wavelengths, which provide both the spectral and spatial information of radicals. As illustrated above, the common methods to record multispectral images are the separation method, the several cameras method, and the consecutive method. Compared with others, separation method is less used in combustion diagnostic due to its high requirements for equipment. The common multispectral imaging method employed in combustion diagnostic is the combination of an ICCD camera and a narrow wavelength filter lens.

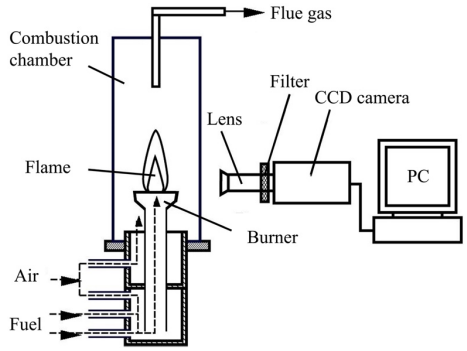

Fig.5. The setup of multispectral imaging method for equivalence ratio measurement. [9]

The setup of the multispectral imaging method for equivalence ratio measurement is shown in Fig.5. The experimental apparatus included a combustion chamber and a ICCD camera equipped with an added filter lens. For this method, the flame should be assumed to be steady because the images are taken one after one. The band-pass filter allows only the signal in that band to pass and be imaged by the ICCD camera. Thus, the multispectral images contain both spectral and spatial information of flame radical, which provides the possibility to analyze the spatial structure of flames. The accuracy of the radical spectral intensity obtained from multispectral image is not precise compared with the spectrum analysis method, because the multispectral image is the integration of the narrow wavelength employed. Based on the advantage of the multispectral imaging method as mentioned above, not only the correlation between combustion characteristics and radical chemiluminescence, but also the correlation between combustion characteristics and radical spatial distribution can be analyzed.

Yang et al. [3] applied the multispectral imaging method in investigating the effects of equivalence ratio variation on the radical distribution and chemiluminescence intensity of OH* and CH* in CH_4/O_2 diffusion flames. The combustion progress in this study was relatively stable, and a mean image was obtained by averaging 15 independent images for further study. The chemiluminescence intensity and distribution of radical are shown in Fig.6. Based on the advantage of multispectral imaging that both the spectral and spatial information can be analyzed, it was found that both the distribution and chemiluminescence intensity of OH* are more significant to vary with the variation of equivalence ratio compared with CH*, and the peak intensity ratio of OH* and CH* decreases linearly with the increase of equivalence ratio.

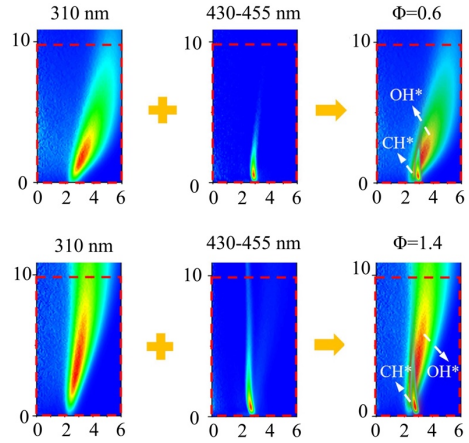

Fig.6. Multispectral image of OH^* and CH^*. [3]

Baumgardner et al. [16] applied the multispectral imaging method to detect the equivalence ratio of premixed propane-air flame from 0.7 to 1.4, and they found that the variation of OH^*/CH^* and C_2^*/CH^* ratio had a good correlation with the increase of equivalence ratio. Based on this, Baumgardner further discovered that equivalence ratio of lean flames was better correlated with OH^*/CH^* ratio, and equivalence ratio of rich flames was better correlated with C_2^*/CH^* ratio. The comparison of OH^*/CH^* and C_2^*/CH^* as they relate to equivalence ratio is shown as Fig.7. Inevitably, the multispectral imaging method loses a certain amount of spectral accuracy because it takes the narrow wavelength filter which contains the whole spectral information in this wavelength. Benefitting from the ability of multispectral imaging method to analyze the spatial information of the flame, Song et al. [17] applied high-spatial-resolution UV imaging equipment to investigate the OH^* characteristic emission and structure of impinging reaction region. As in [18], He et al. investigated the OH^* distribution characteristics under different global oxygen-fuel equivalence ratio, and OH^* chemiluminescence can be employed to characterize the combustion condition appropriately. Fei et al. [8] also applied the multispectral

method in investigating the OH^* chemiluminescence characteristics in CH_4/O_2 lifted flames. Fei et al. imaged the flame with a CCD camera with a band-pass filter lens added and performed the Abel transform [19] on the multispectral image to obtain the OH^* chemiluminescence distribution more precisely. In this study, the differences on lifted flame structure between equivalence ratio and plate-to-nozzle distance is presented.

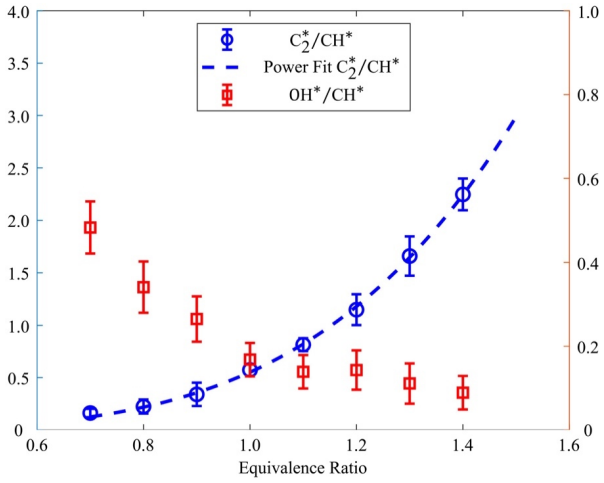

Fig.7. The comparison of OH^*/CH^* and C_2^*/CH^* as they relate to equivalence ratio. [16]

As mentioned above, the multispectral imaging method has a great advantage of obtaining both chemiluminescence intensity and spatial distribution of radicals. This helps in studying the association of flame structure and radical chemiluminescence intensities. But the drawback of the multispectral imaging method is also obvious compared with the spectrum analysis method, that accuracy of the spectral intensity is insufficient because the spectral intensity of the flame is the result of wavelength integration of the filter used. Thus, based on this, some scholars applied both spectrum analysis method and multispectral imaging method in combustion diagnostics. Then, spatial dimension is resolved with multispectral image, and the other dimension of spectrometer resolves for spectrum, providing both spatial and spectral high-resolution. As in [9], Navakas et al. employed both spectrum analysis method and multispectral imaging method to obtain the flame radical emission spectroscopy, in which case the flame chemiluminescence intensity profiles were more precise compared with the single multispectral imaging method. Meanwhile, the radical concentration distribution was obtained, which contributes to investigate the effect of equivalence ratio variation on flame structure.

C. RGB imaging method

Light is an electromagnetic wave with properties as amplitude, wavelength, and frequency. Color is the result of the perception of visible light by the human visual system. The perceived color is determined by the wavelength of the light, which is measured in nanometers. The light with the wavelength in range of 400 nm to 760 nm can be perceived by the human visual system. Huang et al. [10] investigated that the average intensity of B and G channel is well approximate to the radical chemiluminescence intensity of CH^* and C_2^*. To be precise, each pixel of flame image is equipped either with R, G or B filter and the color image is interpolated from this information. The filters are chosen to reproduce human color vision, and how well they suit the radical spectral intensity ratio is purely coincidental. Due to R, G and B filters, the color camera is blind to OH^* chemiluminescence, which is sensitive to the equivalence ratio variation. An additional drawback is that the RGB imaging method loses a lot of sensitivity compared with monochrome cameras.

The setup of the RGB imaging method for equivalence ratio is shown as Fig.8. The RGB imaging system applies the RGB camera to image the flame in the combustion chamber. The setup of the RGB imaging method is simpler compared with the spectrum analysis method and the multispectral imaging method. However, the accuracy of the equivalence ratio measurement is lowest compared with the spectrum method and the multispectral imaging method. The RGB image is the integration of the spectral signal on the broad wavelength which covers several hundred nanometers. But the flame structure is most complete by the RGB imaging method compared with other measuring methods.

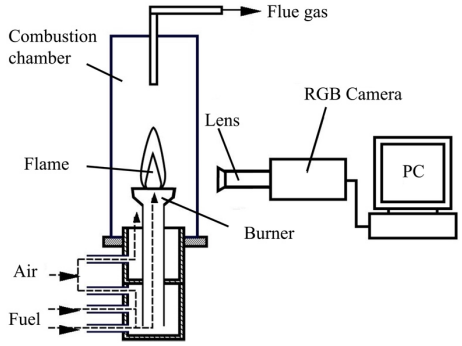

Fig.8. The setup of the RGB imaging method for equivalence ratio measurement.

For RGB pictures imaged by color cameras, the RGB triplet of each pixel reflects the intensity of the spectrum at the corresponding wavelength. The RGB picture of flames under different equivalence ratios is shown in Fig.9. (upper). Based on the thesis proposed by Huang et al. [10], Yang et al. [11] improved the equivalence ratio measuring method based on the color model that established an improved model that pivoted the relationship between flame chemiluminescence and image. The improved corresponding color-modelled CH^*/C_2^* maps at condition (Φ=0.93 – 1.53) are plotted in Fig.9 (lower).

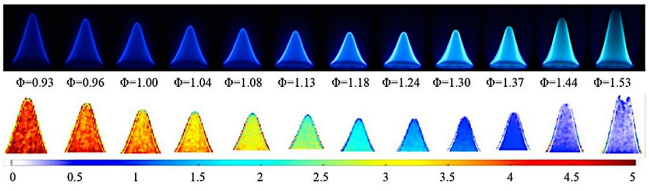

Fig.9. The RGB images of flames under different equivalence ratios (upper) and the corresponding color-modelled CH^*/C_2^* maps. [11]

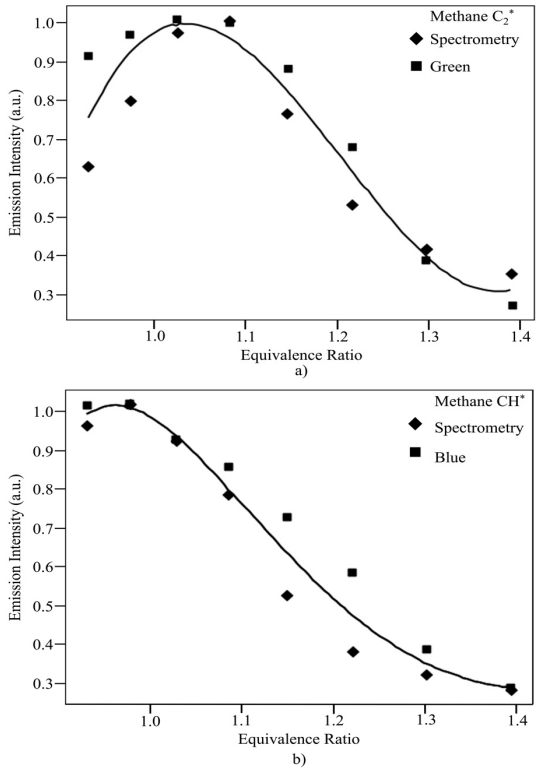

Fig.10. The correlation between radical chemiluminescence and equivalence ratio: a) The chemiluminescence intensity of C_2^*, and the average of G channel with different equivalence. [10]. b) The chemiluminescence intensity of CH^* and the average of B channel with different equivalence.

Huang et al. [10] found that each flame has a distinct spatial distribution in its respective color space, based on which Huang et al. further investigated that the average intensity of the B and G channels in the RGB model can be well approximated to the radical chemiluminescence intensity of CH^* and C_2^*. The relationship between the color and chemiluminescence intensity is shown in Fig.10. On this basis, Huang [20] analyzed the flame characterization based on the RGB imaging method, obtaining the flame chemiluminescence properties through the filtering structure inherent in digital flame images and comparing it with spectrum and laser methods. In this study, Huang et al. investigate that the digitized primary color output is comparable to the radicals in the flame of CH_4 + Air and C_2H_4 + Air. This unique radiation signature makes it possible for the RGB imaging method to be widely applied in combustion diagnostics. Huang et al. [21] applied this method in investigating the dynamic properties of flame to use the Fourier transform to extract the oscillation frequencies from high-speed image of flames, in which case they found that bilateral frequency can be analyzed to assess the different emission state according to the features of diffusion flame and premixed flame. Huang et al. [22] conducted an experimental study of the emission characteristics of flames during the ignition-propagation process of the flame, conducting the ignition tests on an atmospheric burner and an industrial gas turbine burner, respectively, and approximating the high-speed camera as a hyperspectral imaging system to analyze the features of the flame throughout the ignition process. Eventually, Huang et al. found that the beginning of the combustion process started with a normally unobservable color feature which demonstrated the great potential of image-based combustion diagnostics. Yang et al. [23] applied the RGB imaging method in investigating the oscillating flames in an open pipe to detect the chemiluminescence intensity of CH^* and C_2^*, which is produced in the process of propane flame burning, to monitor the fluctuations of the flame and its effects on the chemiluminescence intensity of radicals. It was found that a self-induced fluctuation came into being when the flame passed through an open channel at both ends. It was also found that the fluctuations of the flame increased as the flame propagated after photographing the fluctuations of a propane rich flame in a quartz tube with the equivalence ratio at 1.1 – 1.4. The ratio of the chemiluminescence intensity of CH^* and C_2^* decreased when the flame was pulled back into combustion mixture, and it increased when the flame progressed.

The RGB imaging method is simple to measure the equivalence ratio of the flame, but the accuracy of the method is not so good because the RGB image is the result of integration of the spectral signal over three broad wavelengths. The spectral intensity of the specific radical is difficult to decouple. The drawbacks of the RGB imaging method are that it is blind to OH* chemiluminescence and lacks lots of sensitivity, which makes it difficult to be employed in sites with high accuracy requirements.

3. ACTIVE MEASURING METHODS

Lasers are widely used in combustion diagnostics. The active measuring methods include Laser-Induced Fluorescence (LIF) [24], Planar Laser-Induced Fluorescence (PLIF) [25], Laser-Induced Breakdown Spectroscopy (LIBS) [26], Laser Raman Scattering (LRS) [27], etc. This paper focus on LIF, PLIF, LIBS, and LRS. Compared with the passive measuring method of equivalence, active measuring method has higher accuracy, sensitivity, and spatial resolution, which helps in studying the structure and the concentration of components of flame. A drawback of LIF is that not only a powerful laser source, but also a wavelength is needed to excite fluorescence, and often a frequency-quadrupled Nd: YAG at 266 nm is used. Several complex issues also need to be considered for LIF, since the particles in the excited state are subject to many collisions before they radiate photons. The collisions cause the excited particles to return to the ground state without radiative leap, i.e. quenching, which reduces the efficiency of fluorescence production. Issues such as these further complicate the fluorescence spectrum. Similarly, the lifetime of LIBS signal is very short after the laser excitation. The plasma cools down rapidly, and the atoms recombine to molecules, which leads to a different spectrum and the luminescence ceases finally.

A. Laser-induced breakdown spectroscopy method

Over the past few years, the LIBS method has been widely applied to combustion diagnostic. The equivalence ratio can be measured by detecting the atomic species concentrations in flames. The setup of laser-induced breakdown spectroscopy method for flame equivalence ratio

measurement is shown in Fig.11.

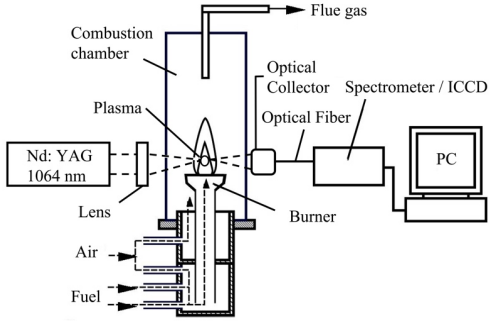

Fig.11. The setup of the LIBS method for flame equivalence ratio measurement.

The basic of LIBS is to apply an optical system to focus the pulsed laser on the surface of the target material and interact with it. The atoms, molecules, etc. within the focused laser spot area absorb the laser energy and undergo multiphoton ionization to produce plasma. Thereafter, the atoms and ions of plasma release the light at specific wavelength and form the corresponding atomic and ion characteristic emission spectra while the atoms and ions in the excited state leap from high energy level to low energy level. However, the lifetime of the LIBS signal is short after excitation. The plasma cools down rapidly, and the atoms recombine to molecules which leads to a different spectrum. Finally, the luminescence ceases.

Based on the wavelength of the characteristic emission spectra and the quantitative relationship between the concentration of the elements and the intensity of the characteristic emission spectra, the qualitative and quantitative information of the elements can be obtained. The intensity of the emission spectra [28] is defined as:

$$I_{ij} = \frac{hc}{4\pi\lambda_{ij}} N_s A_{ij} \frac{g_j}{U^s(T)} \exp(-E_j/k_B T) \quad (2)$$

Here the I_{ij} denotes the intensity of the emission spectra, h denoting the Planck constant (eVs), c denoting the light speed ($m \cdot s^{-1}$), λ_{ij} and A_{ij} denoting the wavelength (nm) and transition probability (s^{-1}), N_s and $U^s(T)$ denoting the particle density and the partition function of particle s, E_j denoting the energy level of the characteristic emission spectra (eV), g_j denoting the statistical weight, k_B denoting the Boltzmann constant ($eV \cdot K^{-1}$), and T denoting the temperature of plasma.

Cremers et al. [29] applied laser-induced breakdown spectroscopy (LIBS) in analyzing the elements in soil firstly and then LIBS was widely used in analyzing the elements of various materials. For the measuring of the equivalence ratio, Michalakou et al. [30] applied LIBS in measuring the partial equivalence ratio of methane, ethylene, and propane combustion with air. As shown in Fig.12., Michalakou took a spectrometer and an ICCD detector into measuring the spectrum of the plasmas in the flames. In this study, Michalakou found that the emission spectra of C, H and O could be used to determine the partial equivalence ratio accurately and a good linear correlation was found between the intensity ratio of the element features.

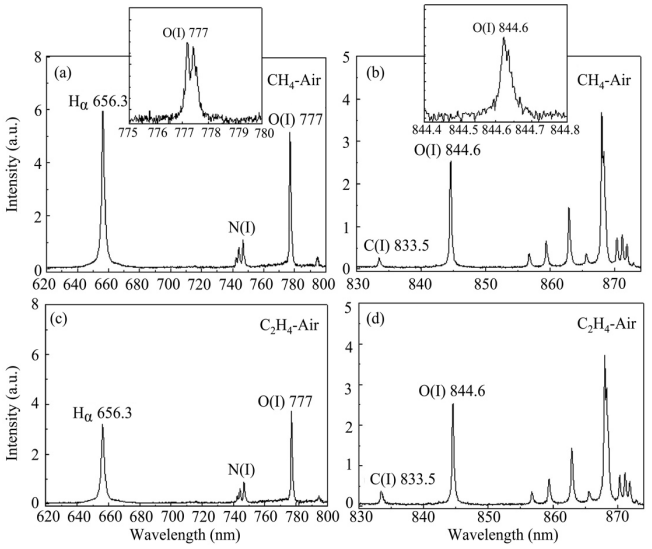

Fig.12. LIBS spectrum of rich laminar premixed: a) and b): methane-air flame (Φ=1.26). c) and d): ethylene-air flame (Φ=1.4). [30]

Due to the limitation of spectrometer, the LIBS spectrum obtained by spectrometers is a one-dimensional signal which does not contain the spatial informational of the flame. Based on the drawbacks, some scholars applied the ICCD camera into imaging the plasma, in which case both the LIBS spectrum and atoms species concentration distribution can be obtained. In [31], Badawy et al. applied LIBS in measuring the lean partially premixed turbulent flame equivalence ratio. And Badawy et al. utilized LIBS to characterize and quantify the impact of changing the disk slit diameter on the distribution profiles of equivalence ratio for the flame. Consequently, as shown in Fig.13., they studied the relationship between the elemental intensity ratio of H/N, H/O and C/N+O, and the equivalence ratio for the premixed NG/air mixture. The accuracy of the LIBS for flame equivalence ratio measurement is relatively high and the spatial information can be analyzed too.

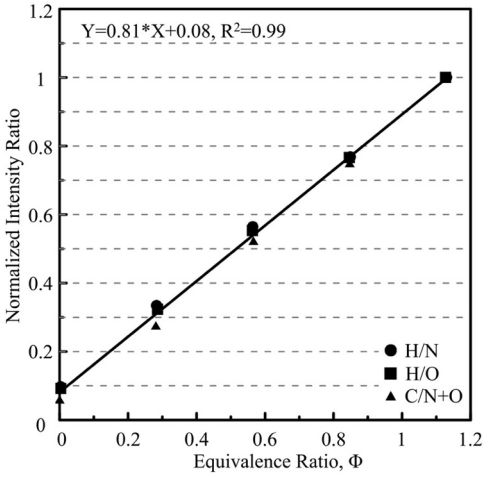

Fig.13. The correlation between the elemental intensity ratio of H/N, H/O and C/N+O, and the equivalence ratio for the premixed NG/air mixture. [31]

B. Planar laser-induced fluorescence method

LIF applies the specific wavelength of laser to excite the components generated in the combustion process. The components are excited to high energy levels after absorbing the energy of laser photons, while the particles emit LIF signals with spectral characteristics when they return to low energy level. The precise information of flame such as components concentration, spectral intensity, etc. can be obtained with the analysis of LIF signals. The laser single pulse fluorescence signal S_F measured in the LIF experiment is formed as:

$$S_F=BI_L\Gamma\tau_L N f_B \Phi F_{fl}\frac{\Omega}{4\pi}\varepsilon\eta V \tag{3}$$

where B is the Einstein absorption coefficient divided by the speed of light, I_L is the laser power spectral density per unit area divided by the laser bandwidth, Γ is the convolution between the excitation and absorption linewidths, τ_L is the laser pulse width, N is the number of molecules in the ground state of the electrons, f_B is the fluorescence quantum that yields the excited state, and F_{fl} is the share of fluorescence collected in the detector band width. The remaining terms, Ω, are the steric angle of the fluorescence collected by the detector, ε and η are the transmission and photoelectric efficiency of the detector, respectively, and V is the volume of the action zone. It should be noted that this equation only applies to the linear region, i.e. when the $BI_L\Gamma$ is small enough, only a small fraction of the particles in the ground state are excited. For LIF, fluorescence quantum yield usually depends strongly on temperature.

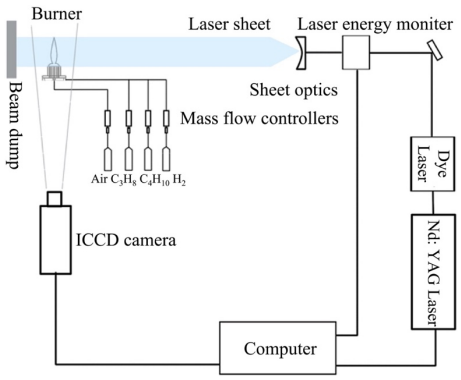

Fig.14. The setup of the PLIF system. [32]

LIF can be applied in measuring the important characteristic parameters in combustion diagnostic due to its advantages of high resolution, high sensitivity, etc. On the other hand, LIF can provide the detailed excitation spectrum which lacks the spatial resolution. Based on it and the limitation of LIF itself, some scholars proposed planar laser-induced fluorescence (PLIF), which is based on LIF, in order to obtain the two-dimensional image of LIF. Scholars use optical lens sets to turn laser beam into light sheet, which is applied to construct PLIF. Miao et al. [33] applied PLIF in investigating the distribution and concentration of OH^* in flame which made use of the PLIF property of spatial information analysis. The experimental setup of the study is shown in Fig.14. In practical terms, a drawback of LIF is that a powerful laser source must be employed to illuminate a plane or even a volume, but also a wavelength is needed to excite the fluorescence. Quite often, a frequency-quadrupled Nd: YAG at 266 nm is used.

Compared with LIF, PLIF can image flame structure, fuel distribution and flame temperature with high spatial and temporal resolution. The PLIF method based on molecular tracer is mainly used to obtain the spatial distribution of mixed gas by adding tracer fractions (ketones, benzene, etc.) into the mixed gas. The component concentration, local equivalence ratio, temperature, etc. can be obtained after experimental calibration and data processing [34]. Vandel et al. [35] applied planar laser-induced fluorescence on a tracer (toluene) to study the local equivalence ratio. The local equivalence ratio of the burner is shown in Fig.15., which shows the equivalence ratio distribution from two dimensions.

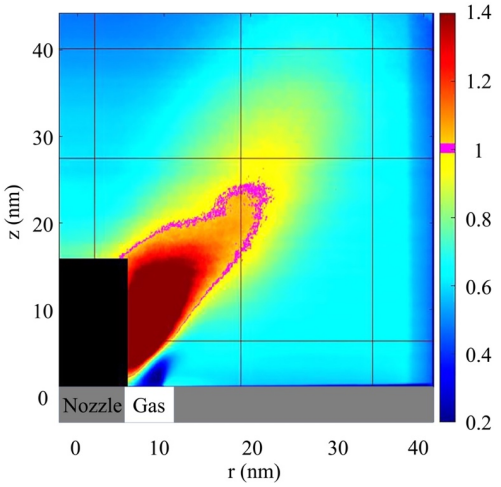

Fig.15. The local equivalence ratio of the burner. [35]

As in [37], for PLIF measurement of equivalence ratio, an aromatic fluorescent tracer (methoxybenzene or anisole) is added to the fuel to mark the field of equivalence ratio. Due to high oxygen quenching, the fluorescent signal of anisole is directly proportional to the equivalence ratio which demonstrates the association of fluorescent signal and equivalence. Peterson et al. [37] also applied the combination of biacetyl planar induced-laser fluorescence and planar particle image velocimetry in measuring the equivalence ratio within the tumble plane of an optical engine. The measuring method proposed by Peterson obtained the fuel number density according to homogeneous fuel fluorescence images which normalized the stratified-fuel fluorescence signal. And the equivalence ratio was calculated from the oxygen concentration and the trapped mass density. Based on the advantage that both radical concentration and distribution can be analyzed, Versailles [38] applied PLIF to measure the concentration of CH^* in the different flames and investigated the correlation between equivalence ratio and CH profile thickness (δ_{CH}), as shown in Fig.16.

Compared with LIF, the PLIF method can both measure the equivalence ratio and obtain the equivalence ratio distribution which helps in further investigating the correlation between the equivalence ratio and other elements of flames.

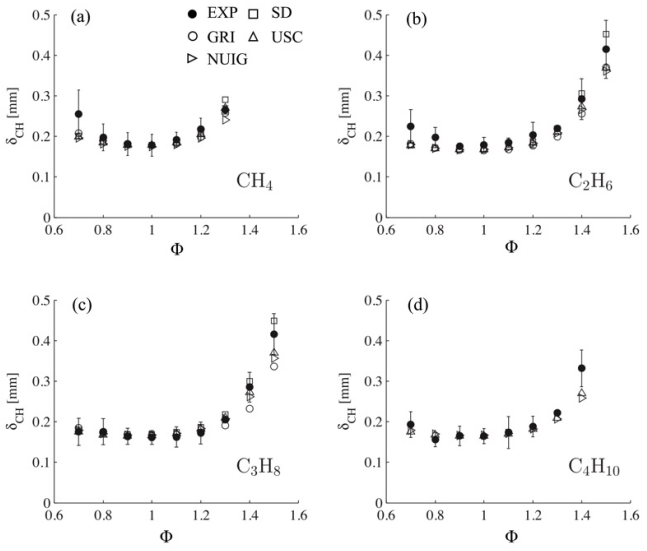

Fig.16. The correlation between equivalence ratio and CH profile thickness. [38]

C. Laser Raman Scattering method

One of the main measurement methods for component concentrations is LRS. When a laser is employed to act on a molecule, it produces Rayleigh scattering and weaker Raman scattering. The Raman spectrum of all components can be obtained with one laser excitation theoretically, which provides the information and Raman spectral intensity of components, and the mole fraction of each component can be calculated. The Raman scattering signal intensity is formed as:

$$S(v, J) \propto n E \frac{g (2J + 1) (v + 1) v_s^4 P_{i,j}}{Q_{rot} Q_{vib}} \exp\left(\frac{[-G_0(v) - F_v(J)] h c}{k T}\right) \quad (4)$$

where V denotes the vibrational quantum number, J denotes the rotational quantum number. T represents the temperature, n represents the molecular concentration, and E is the energy of laser. In addition, $G_0(V)$ and $F_v(J)$ are the vibration and rotation energy spectral terms, respectively, and Q_{vib}, Q_{rot} are the partition functions of the vibrational and rotational energy levels of the molecule, respectively. The g denotes the nuclear spin weight factor of the molecule, and $P_{i,j}$ denotes scattering coefficient of initial and final rotation energy level i and j. The component concentration can be calculated by measuring the Raman scattering signal intensity of the molecule in combustion progress. Wehr [39] employed a 1D-Raman system to measure the major species concentrations, mixture fraction, and temperature in flames. The 1D-Raman experimental setup in [39] is plotted in Fig.17.

Meier et al. [27] employed LRS in concentration measurement in fuel-rich flames, and the emission spectrum was recorded at different equivalence ratios for an excitation as shown in Fig.18. In [40], LRC was applied to investigate the flame behavior and its cyclic variations for the simultaneous determination of the major species concentration and mixture fraction. The experimental setup of LRC is simple and Raman scattering us virtually unaffected by factors such as fluctuations in laser energy. Also, LRS allows simultaneous single-pulse measurements of the major species concentration with high spatial resolution.

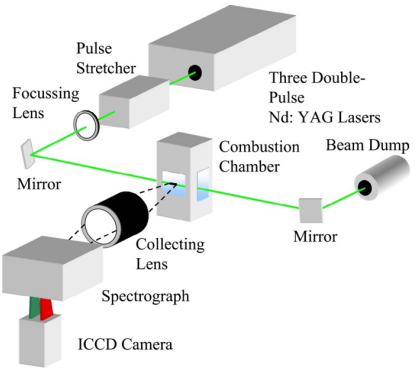

Fig.17. The 1D-Raman experimental setup. [39]

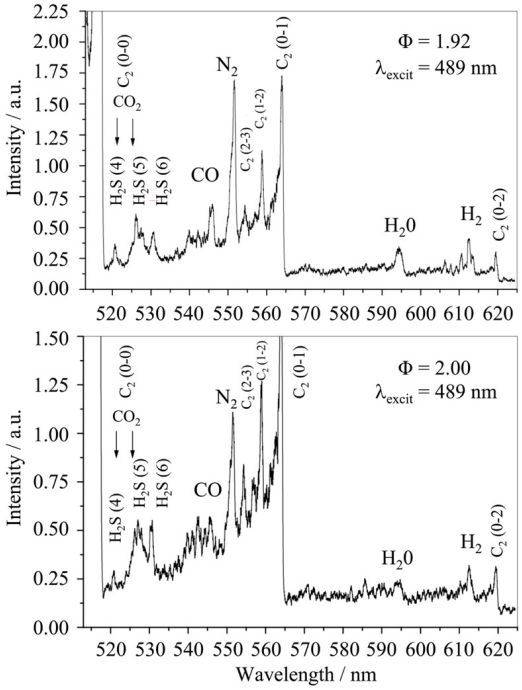

Fig.18. Emission spectra for λ_{exc} = 489 nm. [27]

4. APPLICATIONS OF MACHINE LEARNING

The rapid development of machine learning offers a completely new technological route in the field of combustion diagnostic. Machine learning is widely used in solving various classification, regression, and clustering problems due to its excellent features learning capabilities. The construction of machine learning models generally includes data acquisition, data pre-processing, feature engineering and model training. This paper focuses on the construction of features engineering for the spectral properties of flame radicals and the classifiers which were usually applied in combustion diagnostic.

Feature is a significant factor affecting the accuracy of the model for machine learning and suitable selection of features has contributed to constructing the model accuracy. The spectral characteristics of the flame radicals can be obtained after data acquisition and pre-processing of the flame has been completed, such as one-dimensional spectral signal intensity and two-dimensional multispectral images. From the above, the spectral characteristics of different flame radicals differs from each other, based on which, the feature

engineering can be constructed based on the different radical spectral characteristics.

In general terms, feature is the characteristic variable in a system, which has different values under different conditions. For equivalence ratio measurement based on the spectrum analysis method, the major features, which contribute to indicate the equivalence ratio, are radical chemiluminescence intensity of OH^*, CH^*, and $C2^*$. The traditional modelling approach is that Ordinary Least Square (OLS) is applied to fit the correlation between equivalence ratio and a single variable. In fact, the chemiluminescence intensity of multiple flame radicals changes with the variation of equivalence ratio. Thus, the radical chemiluminescence intensities, which change significantly with the variation of equivalence ratio, should be considered concurrently to construct the model. Different machine learning algorithms such as Multiple Linear Regression (MLR), Random Forest Regression (RFR), Support Vector Regression (SVR), etc. can be applied to construct the model. In reference [41], Vilsen et al. extracted average voltage, standard deviation of voltage, etc. parameters as the features, and MLR was applied to construct the model to predict the battery state-of-health. The fundamental MLR algorithm is formed as (5), where *Xn* is the feature n (radical chemiluminescence intensity) which is an independent variable and *Y* is the equivalence ratio. The β_0 is a common intercept and βn denotes the regression coefficient of feature *n*. However, the limitation of MLR is that MLR requires the correlation between equivalence ratio and each feature to be approximately linear. However, the limitation of MLR is multiple: (1) The correlation between *Y* and *Xn* requires to be approximately linear. (2) The dependent variable should be subject to Gaussian distribution. Thus, the more nonlinear regression models are used in practical application.

$$Y = \beta_0 + \sum_{n=1}^{N} \beta_n X_n + \varepsilon \tag{4a}$$

The one-dimensional spectral signal intensity is the result of the integration of the spectral signal of the target flame region. Thus, the spectral intensity of radicals, ratio of the spectral intensity of different radicals, mean value of spectral intensity, etc. are the identifiable features for feature engineering. Ge et al. [42] analyzed the spectrum of biomass flame over the spectral wavelength from 200 nm to 1200 nm and extracted the spectral intensities of OH^* (310.85 nm), CN^* (390.00 nm), CH^* (430.57 nm) and C_2^* (515.23 nm, 545.59 nm) as the features of biomass flame. After the feature extraction, Ge constructed the identification model including decision tree [43], random forest [44], etc. and enabled the identification for types of biomass fuel. Zhou et al. [45] applied laser-induced breakdown spectroscopy and machine learning algorithms in monitoring the carbon concentration and combustion degree. In this study, the spectral variations of C, O, N, etc. were extracted as the features of kerosene combustion, and the spectral change rule of C in kerosene is plotted in Fig.19.a). The Radial Basis Function (RBF) was employed to perform the combustion degree based on the spectral information, which is suited for nonlinear relationship. The RBF used is a Gaussian kernel function and the distance used was Euclidean distance [46]-[47]. The x denotes the input spectral data, c denotes the center of the kernel function, σ denotes the width parameter of the function which controls the radial range of action of the function. The core idea is that the kernel is applied as hidden unit base to form the implicit layer space, and the input vector is mapped to hidden space directly. The mapping from input to output is nonlinear, and the network output is linear with the adjustable parameters. Based on it, the network weight can be solved from the linear system of equations.

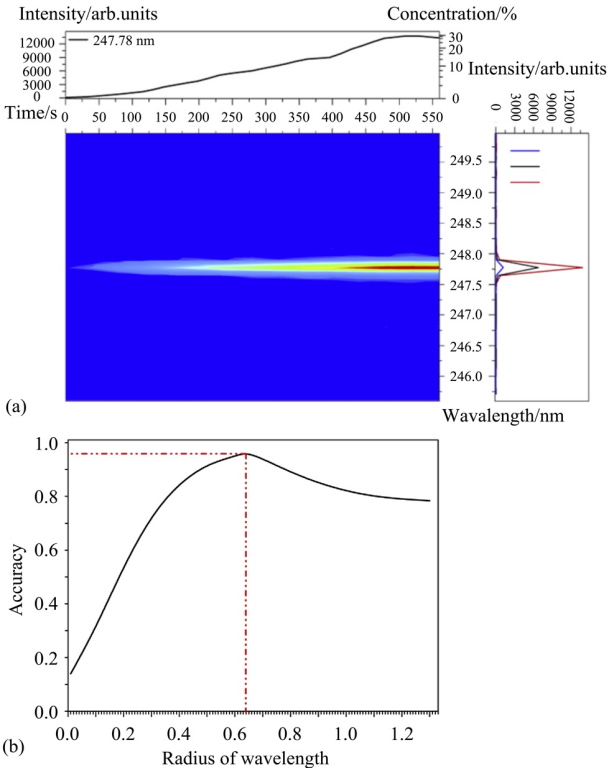

Fig.19. The model accuracy under different wavelength range centered on the carbon spectral peak. [48]

In addition, the influence of different radii of wavelength on prediction accuracy of combustion degree was investigated. Zhou et al. employed the different wavelength range centered on the carbon spectral peak as features and constructed the model based on it, and it indicated that the wavelength range centered on the carbon spectral peak with a radius of 0.64 nm performed best, as shown in Fig.19.b). Thus, it indicates that the quality of feature engineering has a direct impact on the accuracy of the machine learning model. Lee et al. [48] applied laser-induced plasma spectroscopy in analyzing the emission intensity of flame and then normalized the target emission intensity and total spectral intensity. The selected normalized emission intensities were extracted as the features of the flame, and they were trained for the machine learning algorithm as input. It was successful to develop a model which predicted the equivalence ratio. Compared with traditional univariate analysis of the flame features, the method mentioned above fits the multivariate and demonstrates high precision.

Extracting the spectral intensity of flame directly is a simple process and the accuracy of the features extracted is appreciable. But the disadvantage of it is also obvious. The

spectral feature extracted is only the one-dimension data, which lacks the spatial features. Based on it, some scholars extract the features of flame images which include both spectral and spatial information. The spatial features mainly include flame area, height, etc., and the spectral features mainly contain gray value, spectral intensity, etc. Among the features mentioned above, color features can characterize the rich color information of a flame, which is usually constructed with the color moments. The area of target flame in the images is defined as:

$$A = \sum_{i \in R_f} \sum_{j \in R_f} 1, G(i, j) > value \tag{5}$$

where A is the value of the area, R_f is the target area of the flame, and $G(i,j)$ is the gray value of the point (i,j). The brightness of the flame is usually expressed as the normalized average gray value defined as:

$$B = \frac{1}{K} \sum_{i \in R_f} \sum_{j \in R_f} \frac{1}{255} G(i, j) \tag{6}$$

where B is the brightness of the target flame, K is the sum pixel of the target flame, R_f is the target area of the flame, and $G(i,j)$ is the gray value of the point (i,j).

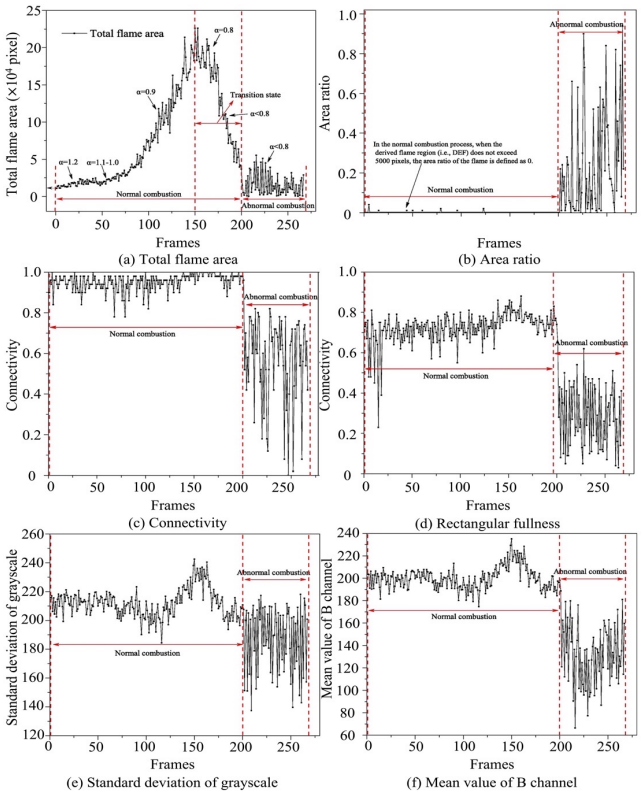

Fig.20. The variation trend of gas fire feature parameters under decreasing equivalence ratio (5 frams/s). a) Total flame area, b) Area ratio, c) Connectivity, d) Rectangular fullness, e) Standard deviation of grayscale, f) Mean value of B channel. [49]

Wang et al. [49] analyzed the difference of gas fire feature parameters under decreasing equivalence ratios, such as total area, gray value, mean value of B channel, etc. Fig.20. shows a combustion process of approximately one minute, where the variation trend of the feature parameters under decreasing equivalence ratio is presented. The steady combustion of gas-fired flame lasts for 40 s, and then the combustion state turns into unsteady state for about 14 s. And five frames were recorded per second, which represents that the frames 0 – 200 are normal combustion and the rest are abnormal combustion. After extracting the image features of gas fire, Wang et al. used the fuzzy pattern recognition algorithm to distinguish the flame burning state. The fuzzy pattern recognition is a classification algorithm based on fuzzy rules which solve the problems with fuzzy properties. The flame burning state recognition method proposed presents a good performance in distinguishing the burning state of flame, and the accuracy of the method is ensured because several feature parameters of flame, which vary with the decreasing of equivalence ratio, are taken into consideration.

For combustion diagnostic, machine learning solves the drawback that traditional data analysis method can only fit the linear relationship, and the multiple features cannot be taken into consideration simultaneously. The accuracy of the machine learning model depends on the quality of feature engineering, and thus the prior knowledge of the characteristic parameters with a sensitive response to the dependent variable is essential.

5. CONCLUSION

The aim of the paper is to provide an overview of the existing equivalence ratio measurement method and the applications of machine learning in combustion diagnostic, and a comparison among different equivalence ratio measurement methods. The existing equivalence ratio measurement methods have been summarized into two main categories: passive measuring methods and active measuring methods. The mechanism, applications, advantages, and limitation have been discussed in detail, which offer a detailed guidance for the suitable selection of a equivalence ratio measuring method.

Among the measuring methods mentioned, spectrum method and laser-induced breakdown spectrum method analyze the spectral information, and thus the accuracy of these measuring methods is ensured. But spectrum method lacks the spatial information of the flame, in which case the structure of flames is difficult to analyze, and LIBS can analyze the concertation distribution of radicals with a CCD camera which is used to image the LIBS signal in combustion. Compared with the measurement method above, planar laser-induced fluorescence provides high spatial resolution as well as high precision. A drawback of LIF is that not only a powerful laser source, but also a wavelength is needed to excite fluorescence, and often a frequency-quadrupled Nd: YAG at 266 nm is used. Multispectral imaging method and RGB imaging method image the spectral signal over narrow wavelength and wide wavelength, both of which are simple to measure the equivalence ratio, but a certain amount of spectrum accuracy is lost. Machine learning can analyze the high-dimensional features, in which case the different features affecting the combustion can be taken into consideration, which solves the problem that the traditional methods of data analysis can only fit a single feature. Thus, machine learning shows a great potential in combustion diagnostic.

ACKNOWLEDGMENT

This work was supported by the Scientific Research Foundation of Guizhou Province (Grant No. 2018[1030]), the Science and Technology Fund of Guizhou Province (No. Qiankehe [2020]1Y266), and Innovation group of Guizhou Education Department (No. Qianjiaohe KY [2021]012).

REFERENCES

[1] Yang, X.F., Yu, M.G., Han, S.X., Qi, B.B. (2021). Effect of equivalence ratio and ignition location on premixed syngas-air explosion in a half-open duct. *Fuel*, 288 (2), 119724. https://doi.org/10.1016/j.fuel.2020.119724

[2] Garcıá-Armingol, T., Ballester, J. (2014). Flame chemiluminescence in premixed combustion of hydron-enriched fuels. *International Journal of Hydrogen Energy*, 39 (21), 11299-11307. https://doi.org/10.1016/j.ijhydene.2014.05.109

[3] Yang, J.B., Gong, Y., Guo, Q., Zhu, H.W., Wang, F.C. Yu, G.S. (2020). Experimental studies of the effects of global equivalence ratio and CO 2 dilution level on the OH* and CH* chemiluminescence in CH 4 /O 2 diffusion flames. *Fuel*, 278, 118307. https://doi.org/10.1016/j.fuel.2020.118307

[4] Kojima, J., Ikeda, Y., Nakajima, T. (2004). Basic aspects of OH(A), CH(A), and C 2 (d) chemiluminescence in the reaction zone of laminar methane–air premixed flames. *Combustion and Flame*, 140 (1-2), 34-45. https://doi.org/10.1016/j.combustflame.2004.10.002

[5] Clark, T.P. (1958). *Studies of oh, co, ch, and c (sub 2) radiation from laminar and turbulent propane-air and ethylene-air flames*. Technical note 4266, National Advisory Committee for Aeronautics, Washington, DC.

[6] Haber, L.C. (2000). *An investigation into the origin, measurement and application of chemiluminescent light emissions from premixed flames.* MS Thesis, Virginia Polytechnic Institute and State University, Blacksbury, VA.

[7] Weber, J.R., Cuccia, D.J., Johnson, W.R., Bearman, G.H., Durkin, A.J., Hsu, M., Lin, A., Binder, D.K., Wilson, D., Tromberg, B.J. (2011). Multispectral imaging of tissue absorption and scattering using spatial frequency domain imaging and a computed-tomography imaging spectrometer. *Journal of Biomedical Optics*, 16 (1), 011015. https://doi.org/10.1117/1.3528628

[8] Fei, X., Yang, J.B., Wei, J.T., Wu, R.M., Song, X.D., Wang, J.F., Yu, G.S. (2021). Investigation of the OH∗ chemiluminescence characteristics in CH_4/O_2 lifted flames. *Journal of the Energy Institute*, 99, 31-38. https://doi.org/10.1016/j.joei.2021.08.007

[9] Navakas, R., Saliamonas, A., Striugas, N., Džiugys, A., Paulauskas, R., Zakarauskas, K. (2018). Effect of producer gas addition and air excess ratio on natural gas flame luminescence. *Fuel*, 217, 478-489. https://doi.org/10.1016/j.fuel.2017.12.094

[10] Huang, H.W., Zhang, Y. (2008). Flame colour characterization in the visible and infrared spectrum using a digital camera and image processing. *Measurement Science and Technology*, 19 (8), 085406. http://dx.doi.org/10.1088/0957-0233/19/8/085406

[11] Yang, J.S., Ma, Z., Zhang, Y. (2019). Improved colour-modelled CH * and C 2 * measurement using a digital colour camera. *Measurement*, 141, 235-240. https://doi.org/10.1016/j.measurement.2019.04.016

[12] Tripathi, M.M., Krishnan, S.R., Srinivasan, K.K., Yueh, F.Y., Singh, J.P. (2012). Chemiluminescence-based multivariate sensing of local equivalence ratios in premixed atmospheric methane–air flames. *Fuel*, 93, 684-691. https://doi.org/10.1016/j.fuel.2011.08.038

[13] Brockhinke, A., Krüger, J., Heusing, M., Letzgus, M. (2012). Measurement and simulation of rotationally-resolved chemiluminescence spectra in flames. *Applied Physics B*, 107 (3), 539-549. https://doi.org/10.1007/s00340-012-5001-1

[14] Vogel, M., Bachfischer, M., Kaufmann, J., Sattelmayer, T. (2021). Experimental investigation of equivalence ratio fluctuations in a lean premixed kerosene combustor. *Experiments in Fluids*, 62, 93. https://doi.org/10.1007/s00348-021-03197-5

[15] Bedard, M.J., Fuller, T.L., Sardeshmukh, S., Anderson, W.E. (2020). Chemiluminescence as a diagnostic in studying combustion instability in a practical combustor. *Combustion and Flame*, 213, 211-225. https://doi.org/10.1016/j.combustflame.2019.11.039

[16] Baumgardner, M.E., Harvey, J. (2020). Analyzing OH*, CH*, and C2* chemiluminescence of bifurcating FREI propane-air flames in a micro flow reactor. *Combustion and Flame*, 221, 349-351. https://doi.org/10.1016/j.combustflame.2020.08.009

[17] Song, X., Guo, Q., Hu, C., Gong, Y. Yu, G. (2016). OH* chemiluminescence characteristics and structures of the impinging reaction region in opposed impinging diffusion flames. *Energy Fuels*, 30 (2), 1428-1436. https://doi.org/10.1021/acs.energyfuels.5b02721

[18] He, L., Guo, Q.H., Gong, Y. Wang, F.C. Yu, G.S. (2019). Investigation of OH* chemiluminescence and heat release in laminar methane–oxygen co-flow diffusion flames. *Combustion and Flame*, 201, 12-22. https://doi.org/10.1016/j.combustflame.2018.12.009

[19] Cho, Y.T., Na, S.J. (2005). Application of Abel inversion in real-time calculations for circularly and elliptically symmetric radiation sources. *Measurement Science and Technology*, 16, 878-884. https://doi.org/10.1088/0957-0233/16/3/032

[20] Huang, H.W., Zhang, Y. (2010). Digital colour image processing based measurement of premixed CH 4 +air and C 2 H 4 +air flame chemiluminescence. *Fuel*, 90 (1), 48-53. https://doi.org/10.1016/j.fuel.2010.07.050

[21] Huang, H.W., Zhang, Y. (2010). Dynamic application of digital image and colour processing in characterizing flame radiation features. *Measurement Science and Technology*, 21 (8), 085202. http://dx.doi.org/10.1088/0957-0233/21/8/085202

[22] Huang, H.W., Zhang, Y. (2011). Analysis of the ignition process using a digital image and colour processing technique. *Measurement Science and Technology*, 22 (7), 075401. http://dx.doi.org/10.1088/0957-0233/22/7/075401

[23] Yang, J., Mossa, F.M.S., Huang, H.W., Wang, Q., Wolley, R., Zhang, Y. (2015). Oscillating flames in open tubes. *Proceedings of the Combustion Institute*, 35 (2), 2075. https://doi.org/10.1016/j.proci.2014.07.052

[24] Lubrano, L.M., Brackmann, C., Capriolo, G., Methling, T., Konnov, A.A. (2021). Measurements of the laminar burning velocities and NO concentrations in neat and blended ethanol and n-heptane flames. *Fuel*, 288, 119585. https://doi.org/10.1016/j.fuel.2020.119585

[25] Soid, S.N., Zainal, Z.A. (2011). Spray and combustion characterization for internal combustion engines using optical measuring techniques – a review. *Energy*, 36, 724-741. https://doi.org/10.1016/j.energy.2010.11.022

[26] Tripathi, M.M., Srinivasan, K.K., Krishnan, S.R., Yueh, F.Y., Singh, J.P. (2013). A comparison of multivariate LIBS and chemiluminescence-based local equivalence ratio measurements in premixed atmospheric methane-air flames. *Fuel*, 106, 318-316. https://doi.org/10.1016/j.fuel.2012.10.079

[27] Meier, W., Keck, O. (2002). Laser Raman scattering in fuel-rich flames: background levels at different excitation wavelengths. *Measurement Science and Technology*, 13 (5), 741-749. http://dx.doi.org/10.1088/0957-0233/13/5/312

[28] He, Y.X., Zhou, W.Q., Ke, C., Xu, T., Zhao, Y. (2021). Review of laser-induced breakdown spectroscopy in gas detection. *Spectroscopy and Spectral Analysis*, 41 (09), 2681-2687. DOI: 10.3964/j.issn.1000-0593(2021) 09-2681-07.

[29] Protopopov, V. (2014). *Practical Opto-Electronics*. Springer, ISBN 978-3319045122.

[30] Michalakou, A., Stavropoulos, P., Couris, S. (2008). Laser-induced breakdown spectroscopy in reactive flows of hydrocarbon-air mixtures. *Applied Physics Letters*, 92 (8), 081501. https://doi.org/10.1063/1.2839378

[31] Badawy, T., Hamza, M., Mansour, M.S., Adbel-Hafez, A.H.H., Imam, H., Adbel-Raheem, M.A., Wang, C.M., Lattimore, T. (2019). Lean partially premixed turbulent flame equivalence ratio measurements using laser-induced breakdown spectroscopy. *Fuel*, 237, 320-334. https://doi.org/10.1016/j.fuel.2018.10.015

[32] Zhu, J.J., Wang, M.G., Wu, G., Yan, B., Tian, Y.F., Feng, R., Sun, M.B. (2021). Research progress of laser-induced fluorescence technology in combustion. *Chinese Journal of Lasers*, 48 (4), 78-110.

[33] Miao, J., Leung, C.W., Cheung, C.S., Huang, Z.H., Jin, W. (2016). Effect of H2 addition on OH distribution of LPG/Air circumferential inverse diffusion flame. *International Journal of Hydrogen Energy*, 41 (22), 9653. https://doi.org/10.1016/j.ijhydene.2016.02.105

[34] Johchi, A., Pareja, J., Böhm, B., Dreizler, A. (2019). Quantitative mixture fraction imaging of a synthetic biogas turbulent jet propagating into a NO-vitiated air co-flow using planar laser-induced fluorescence (PLIF). *Experiments in Fluids*, 60, 82. https://doi.org/10.1007/s00348-019-2723-4

[35] Marrero-Santiago, J., Verdier, A., Brunet, C., Vandel, A., Godard, G., Cabot, G., Boukhalfa, M., Renou, B. (2018). Experimental study of aeronautical ignition in a swirled confined jet-spray burner. *Journal of Engineering for Gas Turbines and Power*, 140 (2), 021502. https://doi.org/10.1115/1.4037752

[36] Balusamy, S., Cessou, A., Lecordier, B. (2014). Laminar propagation of lean premixed flames ignited in stratified mixture. *Combustion and Flame*, 161 (2), 427-437. https://doi.org/10.1016/j.combustflame.2013.08.023

[37] Peterson, B., Reuss, D.L., Sick, V. (2014). On the ignition and flame development in a spray-guided direct-injection spark-ignition engine. *Combustion and Flame*, 161 (1), 240-255. https://doi.org/10.1016/j.combustflame.2013.08.019

[38] Versailles, P., Watson, G.M.G., Lipardi, A.C.A., Bergthorson, J.M. (2016). Quantitative CH measurements in atmospheric-pressure, premixed flames of C1–C4 alkanes. *Combustion and Flame*, 165, 109-124. https://doi.org/10.1016/j.combustflame.2015.11.001

[39] Wehr, L. Meier, W. Kutne, P. Hassa, C. (2007). Single-pulse 1D laser Raman scattering applied in a gas turbine model combustor at elevated pressure. *Proceedings of the Combustion Institute*, 31 (2), 3099-3106. https://doi.org/10.1016/j.proci.2006.07.148

[40] Meier, W., Dem, C., Arndt, C.M. (2016). Mixing and reaction progress in a confined swirl flame undergoing thermo-acoustic oscillations studied with laser Raman scattering. *Experimental Thermal and Fluid Science*, 73, 71-78. https://doi.org/10.1016/j.expthermflusci.2015.09.011

[41] Vilsen, S.B., Stroe, D.-I. (2021). Battery state-of-health modelling by multiple linear regression. *Journal of Cleaner Production*, 290, 125700. https://doi.org/10.1016/j.jclepro.2020.125700

[42] Ge, H., Li, X.L., Li, Y.J., Lu, G., Yan, Y. (2021). Biomass fuel identification using flame spectroscopy and tree model algorithms. *Combustion Science and Technology*, 193 (6), 1055-1072. https://doi.org/10.1080/00102202.2019.1680654

[43] Quinlan, J.R. (1986). Induction of decision trees. *Machine Learning*, 1, 81-106. https://doi.org/10.1007/BF00116251

[44] Breiman, L. (2001). Random forests. *Machine Learning*, 45, 5-32. https://doi.org/10.1023/A:1010933404324

[45] Zhou, Z.Y., Ge, Y.F., Liu, Y.Z. (2021). Real-time monitoring of carbon concentration using laser-induced breakdown spectroscopy and machine learning. *Optics Express*, 29 (24), 39811-39823. https://doi.org/10.1364/OE.443732

[46] Hangelbroek, T., Ron, A. (2010). Nonlinear approximation using Gaussian kernels. *Journal of Functional Analysis*, 259 (1), 203-219. https://doi.org/10.1016/j.jfa.2010.02.001

[47] Shih, F.C., Mitchell, O.R. (1992). A mathematical morphology approach to Euclidean distance transformation. *IEEE Transactions on Image Processing*, 1 (2), 197-204. http://dx.doi.org/10.1109/83.136596

[48] Lee, J.W., McGann, B., Hammack, S.D., Carter, C., Lee, T.H., Do, H., Bak, M.S. (2021). Machine learning based quantification of fuel-air equivalence ratio and pressure from laser-induced plasma spectroscopy. *Optics Express*, 29 (12), 17902-17914. https://doi.org/10.1364/OE.425096

[49] Wang, Y., Yu, Y.F., Zhu, X.L., Zhang, Z.X. (2020). Pattern recognition for measuring the flame stability of gas-fired combustion based on the image processing technology. *Fuel*, 270, 117486. https://doi.org/10.1016/j.fuel.2020.117486

Received December 23, 2021
Accepted February 28, 2022